IMPROVING THE EXTERIOR ORIENTATION OF MARS EXPRESS HRSC IMAGERY

Heinrich Ebner [1], Michael Spiegel [1], Albert Baumgartner [1], Bernd Giese [2],
Gerhard Neukum [3], and the HRSC Co-Investigator Team

[1] Photogrammetry and Remote Sensing, Technische Universitaet, Muenchen, 80290 Muenchen, Germany
spiegel@bv.tum.de, www.remotesensing-tum.de

[2] Institute of Planetary Research, German Aerospace Center (DLR), Rutherfordstr. 2, 12489 Berlin, Germany

[3] Institute of Geosciences, Freie Universität Berlin, Malteserstr. 74-100, 12249 Berlin, Germany
gneukum@zedat.fu-berlin.de

Commission IV, WG IV/9

KEY WORDS: Extra-terrestrial, Three-Line, Sensor, Orientation, Adjustment, DEM/DTM

ABSTRACT

This paper focusses on the estimation of exterior orientation parameters of the High Resolution Stereo Camera (HRSC) orbiting planet Mars during the European Mars Express mission since January 2004. One of the challenges for the photogrammetric processing of HRSC images is the low number of Ground Control Points (GCPs) on Mars which can be identified and measured in the images in the usual way. Therefore, Mars Observer Laser Altimeter (MOLA)-data is employed as control information in the photogrammetric bundle adjustment of HRSC images. A Mars Express specific concept for the photogrammetric point determination and the mathematical model of bundle adjustment with the principle of three-line camera is described. Results are reported for the bundle adjustment with and without MOLA-data as control information.

1 INTRODUCTION

The ESA mission Mars Express with the High Resolution Stereo Camera (HRSC) on board was launched successfully at June 2, 2003 from the Baikonur Cosmodrome in Kazakhstan. In December 2003 the orbiter has arrived at Mars, the orbiting phase started in January 2004 and the first images are acquired. During the first two month of orbiting the HRSC acquired images of an area of about 4 million square kilometers.

The primary goal of the Chair for Photogrammetry and Remote Sensing (LPF) at the Technical University of Munich is to determine the exterior orientation of HRSC orbiting planet Mars during Mars Express mission. In general, the classical photogrammetric point determination requires image coordinates of tie points, interior and exterior orientation, and ground control points (GCP). In case of HRSC on Mars Express tie points will be measured automatically in the images by means of image matching. Interior orientation is assumed to be known from calibration. Observations for the exterior orientation will be derived from star observation, Inertial Measurement Unit (IMU) measurements, and orbit analysis. Unfortunately, these observations for the parameters of the exterior orientation will probably not be precise enough for a consistent photogrammetric point determination on a global level. Nevertheless, they can serve as good approximate values.

Additional control information is necessary in order to fit photogrammetrically derived object points into the existing reference system on Mars. On Mars there are only few precisely known points which can serve as classical GCPs. But there is a large number of ground points measured by MOLA. The special thing about the laser points is, that they can not be identified in the images in an easy way. I.e., image coordinates of most of these points can not be measured, and therefore, it is not possible to treat them as normal GCPs in a bundle adjustment. As a remedy it is proposed to use control surfaces derived from the MOLA points.

In Section 2 the principle of nine-line HRSC, the acquisition of the imagery, and the MOLA-data is described. The concept of photogrammetric point determination with MOLA data as control information in the bundle adjustment is given in Section 3. In Section 4 the first results of HRSC imagery processing are presented and analysed. Section 5 concludes the paper.

2 DATA SOURCES

2.1 High Resolution Stereo Camera (HRSC)

The HRSC (see Fig. 1) is a multi-sensor pushbroom camera consisting of nine Charge Coupled Device (CCD) line sensors for simultaneous high resolution stereo, multispectral, and multi-phase imaging. It has one panchromatic nadir channel, four panchromatic stereo channels, and four channels for color. The convergence angles between the nadir- and the stereo sensors are 21 and 14 gon.

The sensor arrays with 5176 active pixels each are arranged perpendicular to the direction of flight in one focal plane. The images are generated by catenating the continuously acquired line-images. The result is one image per sensor and orbit. One image strip includes all images of one orbit. The pixel size on ground of 12 m will be reached at an altitude of 270 km at pericentre and increase to 50 m at an altitude of 1000 km (Neukum and Hoffmann, 2000).

At pericentre one image strip covers an area of about 60 km across trajectory. In general, the strip has a length of about 300 km up to 4000 km. Figure 2 shows a part of an image from orbit 68.

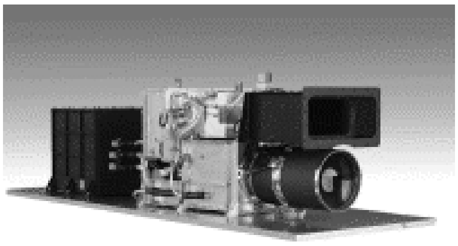

Figure 1: High Resolution Stereo Camera (©DLR, Berlin)

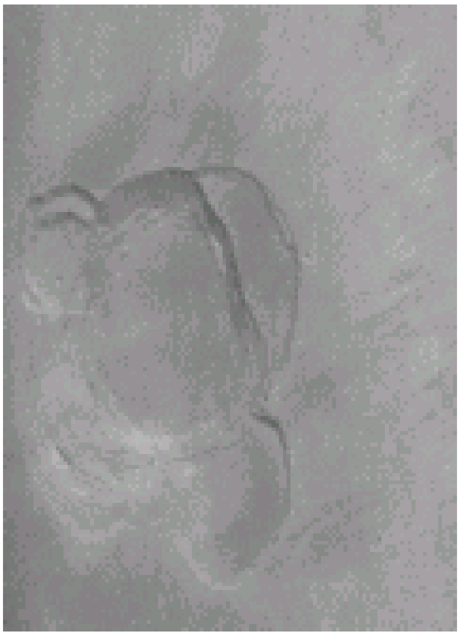

Figure 2: Part of image from orbit 68

In addition to the nine sensors of HRSC, there is another sensor called Super Resolution Channel (SRC). The SRC delivers frame images with 1024 x 1024 Pixel with a ground resolution of 2 - 3 m. This sensor delivers no stereo images. Therefore, a photogrammetric point determination is not possible and the sensor will be not longer considered in this paper.

The three-dimensional position of the spacecraft is constantly determined by the European Space Agency (ESA) applying a combination of doppler shift measurements, acquisition of ranging data, triangulation measurements, and orbit analysis. The orbit accuracy at the pericentre is given as an interval of maximum and minimum accuracy for the whole mission duration (Hechler and Yáñez, 2000). Table 1 shows the accuracy interval for X (direction of flight), Y (perpendicular to the direction of flight), and Z (radial).

X	Y	Z
10 - 2120 m	2.5 - 795 m	1 - 80 m

Table 1: Orbit accuracy at pericentre (Local frame)

The attitude of the spacecraft is derived from measurements of a star tracker camera and from an Inertial Measurement Unit (IMU). The accuracy of the nadir pointing results from a combination of attitude errors and navigation errors. The values for accuracies are 28 mgon for all three angles φ (pitch), ω (roll), and κ (yaw). They are supposed to be valid for the whole mission (Astrium, 2001).

These measurements result in an observed three-dimensional position and attitude of the spacecraft which can be considered as the approximated exterior orientation in classical photogrammetry. However, these observations are not consistent enough for high accuracy photogrammetric point determination.

The interior orientation of the HRSC has been calibrated by Dornier at Friedrichshafen (Carsenty et al., 1997). During the six month journey to Mars the interior orientation has been verified by the means of star observations. So far no deviations from the calibration have been experienced and the interior orientation parameters of the HRSC is considered to be stable.

2.2 Mars Observer Laser Altimeter (MOLA)

In February 1999 the Mars Global Surveyor (MGS) spacecraft entered the mapping orbit at Mars. During the recording time (February 1999 to June 2001) the MOLA instrument acquired more than 640 million observations by measuring the distances between the orbiter and the surface of Mars. In combination with orbit and attitude information these altimeter measurements have been processed to object coordinates of points on the ground. Each orbit results in one track of MOLA points (see Fig. 3).

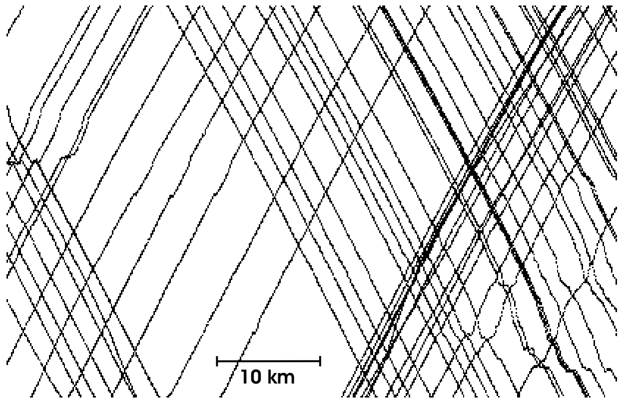

Figure 3: Part of MOLA tracks

The along track resolution is about 330 m with a vertical neighboring precision of 37.5 cm from shot to shot, i.e., from laser point to laser point. The absolute vertical accuracy is in the order of 10 m. The surface spot size is about 168 m in a 400-km-elevation mapping orbit (Smith et al., 2001). The across-track shot to shot spacing depends on the orbit and varies with latitude. In general, the distance between neighboring tracks on the ground is up to more than 1 km (Kirk et al., 2002).

In addition to the surface described by the original, irregularly spaced MOLA track points NASA (Neumann et al., 2003) distributed a grid-based global Digital Terrain Model (DTM) which is derived from these MOLA points (see Fig. 4). The accuracy of DTM is 200 m in planimetry and 10 m in height. As mentioned before, the special thing about the laser points is, that they can not be identified in the images in an easy way. I.e., image coordinates of most of these points can not be measured, and therefore, it is not possible to treat them as normal GCPs in a bundle adjustment.

Figure 4: DTM of Valles Marineris derived from MOLA tracks

3 CONCEPT

In this Section the automated measurement of image coordinates of tie points applying the matching software *hwmatch1* of the Institute of Photogrammetry and GeoInformation (IPI) of University of Hannover and the bundle adjustment software *hwbundle* of LPF will be described.

3.1 Matching

For automatic extraction of image coordinates of tie points software *hwmatch1* is used. Originally, *hwmatch1* was developed at the LPF in Munich for frame images, but the implementation of the extended functional model for three line imagery (Ebner et al., 1994) enabled its use also for line sensor imagery. The IPI modified *hwmatch1* according to the requirements of the Mars Express Mission (Heipke et al., 2004).

As input data the matching needs images, the observed exterior orientation, and the calibrated interior orientation parameters. As an optional input it is possible to use a MOLA DTM as approximate information.

The matching uses feature based techniques. Point features are extracted of the entire images using the Förstner operator. The images of all sensors are matched pairwise in all combinations using the cross correlation coefficient as similarity measure. The results of pixel correlations are sets of image coordinates (coordinate-pairs) of tie points for each image. In addition, the results are refined step by step through different levels of image pyramids.

3.2 Mathematical Model of bundle adjustment

In the bundle adjustment the concept of orientation images proposed by (Hofmann et al., 1982) is used. This approach estimates the parameters of the exterior orientation only at a few selected image-lines, at the so-called orientation images.

The mathematical model for photogrammtric point determination with a three-line camera is based on the well known collinearity equations. These equations describe the fundamental geometrical condition that the rays through the three corresponding image points and the corresponding perspective centers intersect in the object point (see Fig. 5).

Two collinearity equations (Equation (1)) are established for each image point. For every object point there are several equations, because corresponding image points are found in images of different sensors.

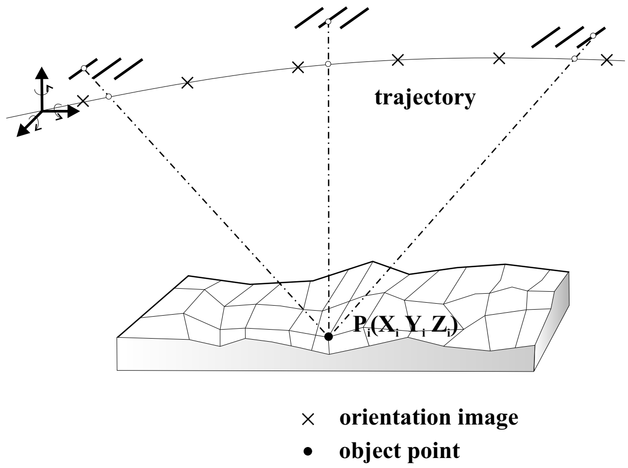

Figure 5: Imaging principle with three line camera

$$
\begin{aligned}
\hat{x}_i &= c\,\frac{\hat{r}_{11}(\hat{X}_i-\hat{X}_0)+\hat{r}_{21}(\hat{Y}_i-\hat{Y}_0)+\hat{r}_{31}(\hat{Z}_i-\hat{Z}_0)}{\hat{r}_{13}(\hat{X}_i-\hat{X}_0)+\hat{r}_{23}(\hat{Y}_i-\hat{Y}_0)+\hat{r}_{33}(\hat{Z}_i-\hat{Z}_0)} \\
\hat{y}_i &= c\,\frac{\hat{r}_{12}(\hat{X}_i-\hat{X}_0)+\hat{r}_{22}(\hat{Y}_i-\hat{Y}_0)+\hat{r}_{32}(\hat{Z}_i-\hat{Z}_0)}{\hat{r}_{13}(\hat{X}_i-\hat{X}_0)+\hat{r}_{23}(\hat{Y}_i-\hat{Y}_0)+\hat{r}_{33}(\hat{Z}_i-\hat{Z}_0)}
\end{aligned}
\quad (1)
$$

$\hat{x}_i, \hat{y}_i$	:	image coordinates of object point P
c	:	calibrated focal length
$\hat{X}_i, \hat{Y}_i, \hat{Z}_i$	:	coordinates of object point P
$\hat{X}_0, \hat{Y}_0, \hat{Z}_0$	:	coordinates of projective center
$\hat{r}_{11}, ..., \hat{r}_{33}$	:	elements of rotation matrix

The collinearity equations are not in linear form and must be linearized by a truncated Taylor's expansion. Therefore, approximations for the orientation parameters and the object points are required in bundle adjustment. All observations are used in a simultaneous least squares adjustment to estimate the unknowns. There are two groups of unknowns, the exterior orientation parameters at few orientation points and the coordinates of the object points. Furthermore, the observations are the image coordinates of object points. The reduced normal equations containing only the unknown exterior orientation parameters shows a band structure. Because of the non-linearity of the problem, several iteration steps are necessary.

3.3 Control Information in bundle adjustment

Starting point of this discussion about DTM data as control information is the approach of (Strunz, 1993). This approach describes the use of DTM as additional or exclusive control information for aerial triangulation. (Strunz, 1993) investigates the conditions for datum determination by exclusive use of DTM. Finally, by means of simulations they analyse the accuracy achievable with DTM as control information which don't have to be identified in the images. Transferring this approach to the case of Mars Express and HRSC means that, the control information is the surface defined by MOLA DTM and HRSC points lie on these surfaces (Spiegel et al., 2003). A drawback of this approach is that it does not use the original MOLA track points but interpolated DTM points. The advantage of this approach is that the effort to search for adequate neighboring MOLA points is reduced because the DTM has a regular grid structure.

Another approach is presented by (Ebner and Ohlhof, 1994), which describes a point determination without classical GCPs, too. Here, as control information they use irregular arranged terrain points which don't have to be identified in the images. Transferred to case of Mars Express (Spiegel et al., 2003), the role of terrain points corresponds to the role of the MOLA track points. However, the HRSC tie points must be acquired in such a way, that at least HRSC points are arranged in the surrounding of each MOLA track point. The HRSC object points would define small surface patches, each containing a MOLA track point.

In principle, these are two viable alternative ways to combine HRSC points and MOLA points. The first approach is to use the terrain surface derived by MOLA DTM points and fit the matched HRSC points into the MOLA surface. The second approach is to use a terrain surface defined by HRSC points and adapt this surface to the MOLA track points which serve as control information. The first alternative is suited better if there are more MOLA points than HRSC points. The second is more reasonable if there are more HRSC points than MOLA points.

The comparison of the matched HRSC tie points and the MOLA data shows that in all investigated areas more MOLA points than matched HRSC tie points are available. Therefore, in the following investigations the first approach will be applied. This approach will be described more in detail now. It uses a least squares adjustment with additional conditions to get a relation between a DTM and the HRSC points. As already mentioned, the HRSC points have to lie on a bilinear surface defined by four neighboring MOLA DTM points, which enclose the HRSC point (see Fig. 6). This condition can be formulated as a constraint on the vertical distance d from the HRSC point to the bilinear surface. Furthermore, this constraint can be substituted by a fictive observation, used as additional observation in the bundle adjustment.

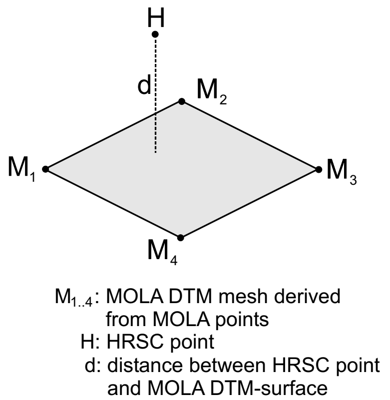

Figure 6: Fitting HRSC point in bilinear surface defined by MOLA DTM

The mathematical model for this observation equation is given in (Equation (2)).

$$\hat{v}_d + d = f(\hat{X}_H, \hat{Y}_H, \hat{Z}_H, X_{M_i}, Y_{M_i}, Z_{M_i}) \qquad (2)$$

For each equation the number of unknowns is three ($\hat{X}_H, \hat{Y}_H, \hat{Z}_H$). It contains one observation ($d = 0$) and twelve constants ($X_{M_i}, Y_{M_i}, Z_{M_i},\ i = 1...4$). The standard deviation σ_d will be determined by the standard deviations of four MOLA DTM points M_1, M_2, M_3, and M_4. Thus, the implementation of the least squares adjustment with observation equations only is quite easy.

With this approach an improvement of the height (Z) can be expected, of course. An improvement in planimetry (X, Y) can only be determined, if there are different local terrain slopes at the different MOLA surfaces.

4 PROCESSING OF HRSC IMAGERY

This section is divided in two parts. Section 4.1 describes the results of bundle adjustment without control information. The results of bundle adjustment with the MOLA DTM as control information is presented in Section 4.2. In both cases the a priori accuracy has been introduced into the bundle adjustment with a value of 1000 m for the position and 28 mgon for the attitude. One whole trajectory of the orbiter is considered to be very stable. Therefore, only a bias over the whole trajectory will be improved. The MOLA DTM is introduced with an accuracy of 100 m instead of 10 m in order to cope with differences between HRSC object points and MOLA track points due to the limited spatial resolution of MOLA. As mentioned before, the resolution on ground of HRSC is up to 12 m compared to the MOLA surface spot size of about 168 m. Regarding local areas, the MOLA data describe the surface less detailed as HRSC object points. The orbits 18, 22, and 68 will be analysed.

4.1 Bundle adjustment without DTM

In order to evaluate the quality of the matched image coordinates, the ray intersections of the tie points are analysed. First the observed values of the exterior orientation are fixed in the bundle adjustment, i.e., they are regarded as error free, and no DTM as control information is introduced. This can be considered as a forward intersection. The obtained values are then compared to the results calculated by the bundle adjustment improving φ and κ. More precisely, a constant bias is modelled for both angles along the entire orbit. In all orbits the number of HRSC points is very high. Thus, it is possible to use only 3-ray points in the bundle adjustment. With 3-ray points the redundancy for each HRSC object point is high and gross errors of image coordinates are visible. These errors can be eliminated by a robust adjustment.

In Table 2 the accuracies of the object coordinates derived from the ray intersections are shown for the selected orbits. The left value is the accuracy of the ray intersections keeping the observed exterior orientation fixed. The right value shows the achieved accuracy of the ray intersections after improving φ and κ, i.e., after estimating the bias in φ and κ.

orbit	altitude [km]	σ_X [m]	σ_Y [m]	σ_Z [m]
18	275 - 347	11 / 5.9	13 / 6.6	34 / 18
22	311 - 941	13 / 7.8	18 / 9.2	42 / 22
68	269 - 505	30 / 10	27 / 11	49 / 18

Table 2: Object point accuracies of ray intersections

The accuracies of the object points for all processed orbits are in a range of about 6 to 11 m in X and Y, depending on different imaging altitudes. Z accuracies for all orbits are about 18 - 22 m. The standard deviations of the ray intersections are improved by a factor of 2 and a final accuracy of about 0.4 pixel on the ground in X and Y and 0.8 pixel in Z is achieved. The generated tie points are evenly distributed over the whole image block except for areas with a lack of texture (see Fig. 7). Black points are 2-ray points and gray points are 3-ray points. White areas are without tie points.

4.2 Bundle adjustment with DTM

The second part of the results shows the evaluation after HRSC object points have been fitted to the MOLA DTM. Here, all six parameters of the exterior orientation ($X_0, Y_0, Z_0, \varphi, \omega, \kappa$) have been improved along the trajectory. The reliability is very high because the coordinates of one point is determined on two ways.

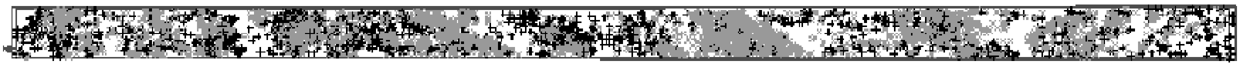

Figure 7: Plot of the generated tie points in orbit 18

On the one hand there is the point determination of HRSC points with three ray points and on the other hand there is the MOLA DTM observation. Under these circumstances the differences between HRSC object points and MOLA DTM can be found. Finally, the MOLA DTM in these areas can be eliminated with a robust adjustment.

orbit		X_0[m]	Y_0[m]	Z_0[m]
18	bias	90.4	-64.6	-38.2
	σ	7.3	11.0	1.6
	bias / σ	12	6	24
22	bias	-300.5	-183.9	-81.8
	σ	24.5	39.5	3.5
	bias / σ	12	4.7	23
68	bias	-12.1	-112.3	-41.2
	σ	10.7	16.7	6.7
	bias / σ	1.1	7	6

Table 3: Accuracies of orbit determination (position bias)

orbit		φ[mgon]	ω[mgon]	κ[mgon]
18	bias	-51.1	-64.4	-6.2
	σ	0.3	1.5	0.1
	bias / σ	194	4.2	63
22	bias	-70.1	-26.3	-8.9
	σ	0.5	2.7	0.7
	bias / σ	164	10	13
68	bias	-24.9	-12.1	-35.9
	σ	0.4	1.9	0.6
	bias / σ	64	11	57

Table 4: Accuracies of orbit determination (attitude bias)

Table 3 and 4 show the improved bias and bias accuracies σ of the positions and attitude for three orbits. In most cases the values can be determined highly significant, because the bias accuracies are lower than the bias values. In orbit 18 the planimetric accuracy σ of the bias is better, because the terrain is rougher.

The accuracies of the coordinates of the object points for the orbits 18, 22, and 68 are shown in Table 5. They depend mainly on two factors. First, there are the accuracies of the ray intersection (Tab. 2) determining the accuracies within the orbit itself. Second, there are the accuracies of the absolute orientation between orbit and MOLA DTM (Tab. 3, Tab. 4). Thus, the precision of the point determination is a combination of these both accuracies. The absolute accuracies of the object points in all three dimensions are less than 20 m for orbit 18 and 68. As a consequence of the higher altitude the result for orbit 22 is slightly worse.

orbit	σ_X [m]	σ_Y [m]	σ_Z [m]
18	9.1	10.6	17.0
22	25.6	35.4	20.9
68	14.4	16.7	17.5

Table 5: Accuracies of HRSC points fitted to MOLA DTM

Finally, Table 6 shows RMS differences in Z between object coordinates of HRSC tie points and MOLA DTM. In one case the result is computed without DTM as control information and in the other case with DTM information. The RMS differences in Z between DTM and HRSC object points are in the range of 200 m. After the bundle adjustment using DTM control information the RMS differences in Z decrease by a factor of three. This means, the adaptation of HRSC data to the MOLA reference system has succeeded.

orbit	18	22	68
without DTM	177 m	268 m	200 m
with DTM	84 m	56 m	63 m

Table 6: RMS differences in Z

5 CONCLUSION

The results show the potential of the image matching and bundle adjustment approaches to achieve an improved exterior orientation with MOLA DTM as control information. The improvement of the accuracy is significant. The position of the exterior orientation increases from an a priori value of 1000 m to less than 20 m in all three dimensions (Tab. 5). The accuracy of the attitude increases from 28 to 1-2 mgon in all angles. With the MOLA DTM as control information the position and attitude can be improved by an average factor of 30 - 50. Thus, after the bundle adjustment the object coordinates of the tie points have a very high accuracy. Finally, there is a high consistency between HRSC points and MOLA DTM, which constitutes the valid reference system on Mars.

REFERENCES

Astrium, 2001. Mars Express – System Requirements Specification. Vol. MEX.MMT.TN.0519, Astrium.

Carsenty, U., Flohrer, J., Jobs, D., Matz, K., Sebastian, I. and Wesemann, K., 1997. HRSC FM1 and FM2 Calibration Document (Final Report). Technical report, DLR, Institut für Planetenerkundung.

Ebner, H. and Ohlhof, T., 1994. Utilization of Ground Control Points for Image Orientation without Point Identification in Image Space. In: International Archives of Photogrammetry and Remote Sensing, Vol. 30, Part 3/1, pp. 206–211.

Ebner, H., Kornus, W. and Ohlhof, T., 1994. A Simulation Study on Point Determination for the MOMS-02/D2 Space Project using an Extended Functional Model. In: Geo-Informations-Systeme, pp. 11–16.

Hechler, M. and Yáñez, A., 2000. Mars Express – Consolidated Report on Mission Analysis Issue 2.0. ESA.

Heipke, C., Schmidt, R., Oberst, J., Neukum, G. and the HRSC Co-Investigator Team, 2004. Performance of Automatic Tie Point Extraktion Using HRSC Imagery of Mars Express Mission. In: International Archives of Photogrammetry and Remote Sensing, Vol. 35.

Hofmann, O., Navé, P. and Ebner, H., 1982. DPS - A Digital Photogrammetric System for Producing Digital Elevation Models and Orthophotos by Means of Linear Array Scanner Imagery. In: International Archives of Photogrammetry and Remote Sensing, Vol. 24-III, pp. 216–227.

Kirk, R. L., Soderblom, L. A., Howington-Kraus, E. and Archinal, B., 2002. USGS High-Resolution Topomapping of Mars with Mars Orbiter Camera Narrow-Aangle Images. In: International Archives of Photogrammetry and Remote Sensing, Vol. 34, Part 4, pp. 713–722.

Neukum, G. and Hoffmann, H., 2000. Images of Mars. In: R. Pellinen and P. Raudsepp (eds), Towards Mars!, pp. 129–152.

Neumann, G., Lemoine, F., Smith, D. and Zuber, M., 2003. The Mars Orbiter Laser Altimeter Archive: Final Precision Experiment Data Record Release and Status of Radiometry. In: Lunar and Planetary Science XXXIV, Abstract #1978, Lunar and Planetray Institute, Houston (CD-ROM).

Smith, D., Zuber, M., Frey, H., Garvin, J., Head, J., Muhleman, D., Pettengill, G., Phillips, R., Solomon, S., Zwally, H., Banerdt, W., Duxbury, T., Golombek, M., Lemoine, F., Neumann, G., Rowlands, D., Aharonson, O., Ford, P., Ivanov, A., Johnson, C., McGovern, P., Abshire, J., Afzal, R. and Sun, X., 2001. Mars Orbiter Laser Altimeter: Experiment summary after the first year of global mapping of Mars. In: Journal of Geophysical Research, Vol. 106(E10), pp. 23,689–23,722.

Spiegel, M., Baumgartner, A. and Ebner, H., 2003. Orientation of Mars Express/HRSC Imagery Using Laser Altimeter Data as Control Information. In: ISPRS Workshop High Resolution Mapping from Space 2003, Hannover (CD-ROM).

Strunz, G., 1993. Bildorientierung und Objektrekonstruktion mit Punkten, Linien und Flächen. Deutsche Geodätische Kommission (Reihe C, 408), München.

ACKNOWLEDGEMENTS

This work is funded by Deutsches Zentrum für Luft- und Raumfahrt e.V. (DLR) under grant no. 50 QM 0103. This support is gratefully acknowledged.